

# Phase separation and valence instabilities in cuprate superconductors. Effective one-band model approach.

M. E. Simón and A. A. Aligia

*Centro Atómico Bariloche and Instituto Balseiro*

*Comisión Nacional de Energía Atómica*

*8400 Bariloche, Argentina*

## Abstract

We study the Cu-O valence instability (VI) and the related phase separation (PS) driven by Cu-O nearest-neighbor repulsion  $U_{pd}$ , using an effective extended one-band Hubbard model ( $H_{eff}$ ) obtained from the extended three-band Hubbard model, through an appropriate low-energy reduction.  $H_{eff}$  is solved by exact diagonalization of a square cluster with 10 unit cells and also within a slave-boson mean-field theory. Its parameters depend on doping for  $U_{pd} \neq 0$  or on-site O repulsion  $U_p \neq 0$ . The results using both techniques coincide in that there is neither VI nor PS for doping levels  $x < 0.5$  if  $U_{pd} \lesssim 2$  eV. The PS region begins for  $U_{pd} \gtrsim 2$  eV at large doping  $x > 0.6$  and increases with increasing  $U_{pd}$ . The PS also increases with increasing on-site Cu repulsion  $U_d$ .

PACS numbers: 74.72.-h, 74.25.Jb

## I. INTRODUCTION

It is widely accepted that the electronic properties of the cuprates are well described by the three-band Hubbard model  $H_{3b}$  [1–3]. Zhang and Rice [4] suggested that this model can be reduced to an effective one-band  $t - J$  model under certain simplifying hypothesis: small O-Cu hopping  $t_{pd}$ , and zero on-site O Coulomb repulsion  $U_p$ , Cu-O Coulomb nearest-neighbor interatomic repulsion  $U_{pd}$  and O-O hopping  $t_{pp}$ . While the one-band effective models can explain the magnetic properties of high- $T_c$  materials and can provide magnetic mechanisms for superconductivity [5,6], these models, with fixed parameters, do not take into account the effects of the Cu-O repulsion  $U_{pd}$ . The density of carriers in cuprate superconductors is very low. The average distance between two holes is larger than 7 Å and the Cu-O distance is  $\sim 1.9$  Å and therefore  $U_{pd}$  is expected to be poorly screened. Neglecting screening  $U_{pd} \sim 7$  eV, while direct calculations give  $U_{pd} \sim 3$  eV [7] and constrained-density-functional results predict  $U_{pd} \sim 1$  eV [8]. Thus, as pointed out early after the discovery of high- $T_c$  superconductivity, the effects of  $U_{pd}$  can be important [2,9]. These effects include a charge-transfer mechanism for superconductivity [3,9,10], and marginal -Fermi-liquid behavior [11]. It is known that a sufficiently large  $U_{pd}$  induces a charge-transfer instability (CTI) and a valence instability (VI) related with Cu-O charge transfer [12]. These instabilities are associated with phase separation because of the coupling between the fluctuations of the valence and the total density [13,14].

The three-band Hubbard model including  $U_{pd}$  has been studied by exact diagonalization of small clusters [9], random-phase approximation [3,13,15,16], Gutzwiller variational wave function [17], and slave-bosons with 1/N expansion, for the particular case  $U_d = \infty$  and with  $U_p$  and  $U_{pd}$  treated in the Hartree approximation [14,18,19]. The results of these works are qualitatively similar in general. Increasing  $U_{pd}$  the system reaches the CTI, VI and the related phase separation. Near the phase-separation boundary, the effective interaction in the Cooper  $s$  and  $d$  channels becomes attractive.

Bang *et al.* in weak coupling [13] and Raimondi *et al.* in strong coupling [14] have

shown that even though the energy  $\omega_{exc}$  of the charge-transfer collective excitonic mode at zero wave vector, decreases with increasing  $U_{pd}$ , it remains finite at the CTI. However, this mode is coupled to the zero-sound mode, leading to a charge-transfer-mode mediated attraction which allows the violation of the Landau stability criterion  $F_0^S > -1$ . This leads to the simultaneous divergence of the compressibility and charge-transfer static susceptibility indicating that phase separation and the CTI take place.

In spite of the qualitative agreement on the facts mentioned above among the different techniques, the regions of phase separation differ in the strong and weak coupling approaches, and the critical value of  $U_{pd}$  where the instabilities take place depends strongly on the approximation used. Also, the effect of the variation of the parameters has not been investigated in detail and realistic values of  $U_d$  have not been studied so far. Thus, further research on these subjects seems necessary.

On the other hand, it is important to address the question of to what extent the above mentioned properties of the three-band Hubbard model can be accounted for using a one-band effective model derived from the former through a sufficiently accurate mapping procedure. Generalized  $t - J$  and one-band Hubbard models have been obtained performing systematic low-energy reductions of the three-band Hubbard [20–27]. These reductions either are based on a cell method [20,21] or use an effective spin-fermion model with renormalized parameters as an intermediate step in the derivation [27,28]. In contrast to the original derivation of Zhang and Rice, these methods allow to extend the mapping procedure to realistic and large values of Cu-O hopping  $t_{pd}$ , and show that the Zhang-Rice singlets are stable for large Cu-O covalency. There have been an important amount of research devoted to the study of the validity of the low-energy reduction and the stability of the Zhang-Rice singlets. In particular, the roles of local triplets states [29] and apical O ions [30] have been recently investigated. Exact diagonalization of small clusters have shown that the low-energy spectrum [29,31] and magnetic properties [32] of the three-band model can be well reproduced by a  $t - t' - t'' - J$  model, where  $t'$  is the next-nearest-neighbor hopping and  $t''$  is a next-nearest-neighbor hopping combined with a nearest-neighbor spin flip. This three-

body term, with the sign corresponding to large O-O hopping  $t_{pp}$  in the original three-band model, can stabilize a resonance-valence-bond superconducting ground state [6].

In this paper, starting from the three-band Hubbard model, we derive an effective generalized one-band Hubbard model, using the cell method generalized to take into account properly the intercell part of the O intratomic repulsion  $U_p$  and the Cu-O interatomic repulsion  $U_{pd}$ . As a consequence of these interactions, the parameters of the effective model become dependent on the particle density. Solving the effective one-band model exactly in a  $\sqrt{10} \times \sqrt{10}$  cluster, and also in the slave-boson mean-field theory of Kotliar and Ruckenstein [33] we study the above mentioned valence instability (VI), the regions of phase separation (PS), and also the dependence of the effective one-band parameters with  $U_{pd}$  and doping. The advantage of our approach in comparison with other methods discussed above for the study of the VI, CTI and PS, is that the intracell correlations, including Cu on-site repulsion  $U_d$  and a large part of the  $U_{pd}$  and  $U_p$  terms, are taken into account exactly at each cell. This allows us in particular to take realistic values of  $U_d$  ( $\sim 10$  eV), while in previous treatments  $U_d$  was either small or infinite.

In section II we describe the different Hamiltonians and the method for low-energy reduction. Section III contains the results and section IV is a short summary and discussion.

## II. REDUCTION FROM THE THREE-BAND TO A ONE-BAND HAMILTONIAN

We start from the three-band extended Hubbard model:

$$H_{3b} = \Delta \sum_j p_{j\sigma}^\dagger p_{j\sigma} + U_d \sum_i d_{i\uparrow}^\dagger d_{i\uparrow} d_{i\downarrow}^\dagger d_{i\downarrow} + U_p \sum_j p_{j\uparrow}^\dagger p_{j\uparrow} p_{j\downarrow}^\dagger p_{j\downarrow} + U_{pd} \sum_{i\delta\sigma\sigma'} d_{i\sigma}^\dagger d_{i\sigma'} p_{i+\delta\sigma}^\dagger p_{i+\delta\sigma} + t_{pd} \sum_{i\delta\sigma} (p_{i+\delta\sigma}^\dagger d_{i\sigma} + h.c.) - t_{pp} \sum_{j\gamma\sigma} p_{j+\gamma\sigma}^\dagger p_{j\sigma} \quad (1)$$

The sum over  $i$  ( $j$ ) runs over all Cu (O) ions. The vector  $\delta$  ( $\gamma$ ) connects a Cu (O) site with one of its four nearest O atoms. The operator  $d_{i\sigma}^\dagger$  ( $p_{j\sigma}^\dagger$ ) creates a hole with symmetry  $d_{x^2-y^2}$  ( $p_\sigma$ ) at site  $i$  ( $j$ ) with spin  $\sigma$ . The phases of half of the orbitals have been changed in such

a way that for all directions, the hoppings are positive ( $t_{pd}, t_{pp} > 0$ ). The parameters of the model are known approximately from constrained-density-functional calculations [8].

The first step in the cell method [21,24,26] is to change the basis of the O orbitals to linear combinations which hybridize ( $\alpha_{k\sigma}$ ) and do not hybridize ( $\gamma_{k\sigma}$ ) with  $d_{k\sigma}$  orbitals, due to the term in  $t_{pd}$  at each point  $\mathbf{k}$  of the reciprocal space. We denote the Wannier functions of these orbitals as  $\alpha_{i\sigma}$  and  $\gamma_{i\sigma}$  respectively. The  $\gamma_{i\sigma}$  (*non-bonding* states) lie very high in energy and are neglected. After the change of basis, the original Hamiltonian can be separated in two parts, one containing the intracell (and generally larger) terms and another containing the intercell terms:

$$H_{3b} = \sum_i H_i + H_{inter}, \quad (2)$$

with

$$\begin{aligned} H_i = & (\Delta - \mu(0)t_{pp}) \sum_{\sigma} \alpha_{i\sigma}^{\dagger} \alpha_{i\sigma} \\ & + U_d d_{i\uparrow}^{\dagger} d_{i\uparrow} d_{i\downarrow}^{\dagger} d_{i\downarrow} + 2t_{pd}\lambda(0) \sum_{\sigma} (d_{i\sigma}^{\dagger} \alpha_{i\sigma} + h.c.) \\ & + U_{pd}f(0) \sum_{\sigma\sigma'} d_{i\sigma'}^{\dagger} d_{i\sigma'} \alpha_{i\sigma}^{\dagger} \alpha_{i\sigma} + U_p h(0) \alpha_{i\uparrow}^{\dagger} \alpha_{i\uparrow} \alpha_{i\downarrow}^{\dagger} \alpha_{i\downarrow} \end{aligned} \quad (3)$$

$$\begin{aligned} H_{inter} = & \sum_{i \neq j\sigma} [2t_{pd}\lambda(j-i)d_{j\sigma}^{\dagger} \alpha_{i\sigma} - t_{pp}\mu(j-i)\alpha_{j\sigma}^{\dagger} \alpha_{i\sigma} + h.c.] \\ & + U_{pd} \sum_{i \neq j \neq l \sigma \sigma'} [f(i-j, i-l) n_{i\sigma'}^d \alpha_{j\sigma}^{\dagger} \alpha_{l\sigma} + h.c.] \\ & + U_p \sum'_{ijlm} h(i-j, i-l, i-m) \alpha_{i\uparrow}^{\dagger} \alpha_{m\uparrow} \alpha_{j\downarrow}^{\dagger} \alpha_{l\downarrow} \end{aligned} \quad (4)$$

The functions of the lattice vectors  $\lambda, \mu, \nu, f$  and  $h$  are given in Ref. [26]. They decay rapidly with increasing argument and as a consequence, most of the original hoppings and interactions are contained in  $\sum_i H_i$ . The  $\sum'$  indicates that in the last sum the term with  $i = j = m = l$  is excluded.

The ordinary cell method consists in solving  $H_i$  exactly in the subspaces of 0, 1 and 2 particles and retaining the ground state in each subspace. The non trivial retained eigenstates have the form:

$$|i2\rangle = \frac{A_1}{\sqrt{2}}(d_{i\uparrow}^\dagger \alpha_{i\downarrow}^\dagger - d_{i\downarrow}^\dagger \alpha_{i\uparrow}^\dagger) - A_2 \alpha_{i\uparrow}^\dagger \alpha_{i\downarrow}^\dagger - A_3 d_{i\uparrow}^\dagger d_{i\downarrow}^\dagger |0\rangle. \quad (5)$$

$$|i\sigma\rangle = (B_1 d_{i\sigma}^\dagger - B_2 \alpha_{i\sigma}^\dagger) |0\rangle. \quad (6)$$

The energies of these states will be denoted  $E_2$  and  $E_1$  respectively. The first term of  $|i2\rangle$  corresponds to the Zhang-Rice singlet in the original derivation [4]. Our modification consists in considering the coefficients as variational parameters which are determined minimizing the total energy. We treat the terms in  $U_{pd}$  of  $H_{inter}$  with  $i \neq j \neq l$  replacing  $n_{i\sigma'}^d$  by its expectation value. Using the fact that  $\sum_i f(i-j, i-l) = 0$ , this is equivalent to the treatment of Ref. [22]. Similarly in the terms in  $U_p$  of  $H_{inter}$  with  $i = m$  and  $j \neq l$  we replace  $\alpha_{i\sigma}^\dagger \alpha_{i\sigma}$  by its expectation value. The same treatment is done for  $i \neq m$  and  $j = l$ . The remaining terms except those with  $i = m$  and  $j = l$  were neglected. The intercell Hamiltonian is written as a function of the retained eigenstates of  $H_i$ , and mapping the latter into those of the one-band Hubbard model at site  $i$ , one obtains the following effective model:

$$\begin{aligned} H = & E_1 \sum_{i\sigma} n_{i\sigma} + U \sum_i n_{i\uparrow} n_{i\downarrow} + \sum_{<ij>\sigma} (c_{j\sigma}^\dagger c_{i\sigma} \{t_{AA}(1 - n_{i,-\sigma})(1 - n_{j,-\sigma}) \\ & + t_{AB}[n_{i,-\sigma}(1 - n_{j,-\sigma}) + n_{i+l,-\sigma}(1 - n_{i,-\sigma})] + t_{BB} n_{i,-\sigma} n_{j,-\sigma} + h.c. \\ & \sum_{<ij>\sigma\sigma'} V_{11}(1 - n_{i,-\sigma})(1 - n_{j,-\sigma'}) n_{i\sigma} n_{j\sigma'} \\ & \sum_{<ij>\sigma\sigma'} V_{12}((1 - n_{i,-\sigma})n_{j,-\sigma'} + n_{i,-\sigma}(1 - n_{j,-\sigma'})) n_{i\sigma} n_{j\sigma'} \\ & \sum_{<ij>\sigma\sigma'} V_{22} n_{i,-\sigma} n_{j,-\sigma'} n_{i\sigma} n_{j\sigma'} \end{aligned} \quad (7)$$

We obtain the ground state energy of  $H$  as a function of the three free variational parameters (Eqs. 5 and 6) using two different approaches:

1. The slave-boson approximation (SB) of Kotliar and Ruckenstein [25,33] after treating the nearest-neighbor repulsions in the Hartree-Fock approximation.
2. Exact diagonalization (ED) of a square cluster with 10 unit cells.

### III. RESULTS

We begin this section by studying the parameters of the one-band effective model and its dependence with the original parameters and doping. As a basis for our study we take the parameters of the original three-band Hubbard model determined from constrained-density-functional approximation [8]. We take the unit of energy as  $t_{pd} = 1 \simeq 1.3$  eV. However we also study the effect of  $U_{pd}$  and  $U_d$  within a wider range. In the (unrealistic) limit  $U_p = U_{pd} = 0$ , the intercell interactions vanish ( $V_{11} = V_{12} = V_{22} = 0$ ) and the variational parameters  $A_i$ ,  $B_i$  (Eqs. 5 and 6) which minimize the total energy correspond to the eigenstates of the cell Hamiltonian  $H_i$  (Eq. 3) for all dopings. Thus the effective one-band parameters are independent of doping. Increasing  $U_{pd}$  and  $U_p$ , the intercell interactions appear and the variational parameters start to differ from those corresponding to the low-energy eigenstates of  $H_i$  to take into account better the intercell interactions. The variational parameters as well as the one-band effective parameters become doping dependent, although this dependence is very weak for small  $U_{pd}$  and  $U_p$ .

In Figs. 1-4 we show the one-band parameters as functions of doping for different values of  $U_{pd}$  using ED. The effective on-site repulsion  $U$  increases with  $U_{pd}$  except for small values of  $\Delta$  and high doping where the amount of O states in the local singlet (Eq. 5) increases and the mixed Cu-O part (which pays  $\sim U_{pd}$ ) decreases. Related with this fact,  $U$  decreases with doping for small values of  $\Delta$ . This reflects a *metallization* of the system with a larger amount of Cu-O covalency which should be reflected in an increase of the conductivity. This might be related to the sudden increase in the Hall conductivity observed in  $\text{La}_{2-x}\text{Sr}_x\text{CuO}_4$  for  $x > 0.17$  [34]. As a consequence of the larger amount of O holes in the doubly occupied cells, and the change in the variational parameters  $B_i$  (Eq. 6) to minimize the loss of energy due to the Cu-O repulsion  $U_{pd}$ , the energy  $E_1$  and the amount of O holes in the singly-occupied cells increase with doping for small  $\Delta$  and large  $U_{pd}$ . For others values of  $\Delta$  and  $U_{pd}$ ,  $E_1$  is rather insensitive to doping (see Fig. 2).

For small values of  $U_{pd}$  the three correlated hoppings of the effective one-band model are

rather insensitive to doping and similar in magnitude. For large values of  $U_{pd}$  the last two terms in Eq. (4) can not be neglected and affect somewhat the magnitude of these hoppings. As for the case of the correlated hoppings, if  $U_{pd} \lesssim 1$  the different effective nearest-neighbor repulsions are similar between them and rather independent of hopping. However in contrast to the former, the  $V$ 's increase significantly with  $U_{pd}$ . For small  $\Delta$  and large  $U_{pd}$ , in spite of the fact that there is a significant charge transfer from Cu to O with doping, the effective repulsions do not change very much because the decrease (increase) in Cu-O repulsion is approximately compensated by the increase (decrease) in O-O repulsion.

In Figs. 5 and 6 we show the dependence of the expectation value  $n_d = \langle n_{i\uparrow} + n_{i\downarrow} \rangle$  on  $\Delta$ . As expected,  $n_d$  increases with  $\Delta$ . For small  $U_{pd}$  the results obtained by exact diagonalization (ED) and slave bosons (SB) are qualitatively similar, although there are quantitative differences of the order of 20% for larger dopings. For larger values of  $U_{pd}$  there are some important qualitative differences between both methods which are discussed below, however both methods coincide in that for intermediate and small values of  $\Delta$ ,  $n_d$  *decreases* with doping as a consequence of Cu-O charge transfer which overcompensates the effect of doping (see Figs. 6 and 7). This is related with the increase in Cu-O covalency and the *metallization* mentioned before. In contrast, for large values of  $\Delta$ ,  $n_d$  *increases* faster with doping than for small values of  $U_{pd}$ . As a consequence of these opposite effects of  $U_{pd}$  for small and large  $\Delta$ , the dependence of  $n_d$  with  $\Delta$  becomes more abrupt for large  $U_{pd}$ , eventually driving the valence instability (VI). The effect of reducing  $U_d$  induces a larger Cu occupancy  $n_d$  at large values of  $\Delta$  favoring the VI. The static valence susceptibility is defined by:

$$\chi_V = \frac{\partial(n_d - n_p)}{\partial\Delta}|_n = 2\frac{\partial n_d}{\partial\Delta}|_n, \quad (8)$$

where  $n$  is the total occupation per cell and  $n_p = n - n_d$  is the O occupation per cell.  $\chi_V$  differs from the charge-transfer susceptibility  $\chi_{CT}$  because the latter is defined at constant chemical potential instead of at constant  $n$ . The valence susceptibility  $\chi_V$  is shown in Fig. 8. For each value of  $x = n - 1$ , there is a critical value of  $U_{pd}$  ( $U_{pd}^c(x)$ ) for which  $\chi_V$  diverges

at a critical value of  $\Delta$  ( $\Delta^c(x)$ ), indicating the presence of a VI. For  $U_{pd} > U_{pd}^c$  there is a discontinuous transition as shown for example in Fig. 6 for  $x = 0.8$ . The minimum possible value of  $U_{pd}^c(x)$  occurs for maximum doping ( $x = 1$ ). The critical value  $U_{pd}^c(x)$  increases with decreasing  $x$ . Note that  $U_{pd}^c(x)$  found with SB is always lower than that found with ED. Also, at  $x = 0$  the SB approximation gives an artificially large  $\chi_V$  at the metal-insulator transition due to the vanishing of the double occupancy ( $d$ ) in the insulating phase and the exaggerated large increase of  $d$  with  $\Delta$  in the metallic phase near the metal-insulator boundary. Within the ED,  $d$  grows smoothly with  $\Delta$  in absence of the VI as one expects.

In Fig. 9 we show the phase-separation diagram calculated with the SB approximation. Contrary to previous strong-coupling mean-field approximations, where always one of the phases between which phase separation takes place has  $x = 0$  [14], we obtain, in qualitative agreement with weak-coupling approximations [16] that phase separation takes place between a phase with large doping  $x = 1$  and another one with  $x$  depending of the parameters. As expected, the region of phase separation grows with increasing  $U_{pd}$ . At least for  $U_{pd} \leq 1$ , (*i.e.* for parameters near those obtained by constrained-density-functional approximation [8]) there is no phase separation. The effect of decreasing  $U_d$  on phase separation is to suppress it for large values of  $\Delta$ . This is related with the change of the character of the local singlet  $|i2\rangle$  (Eq. 5) from mainly Cu-O or O-O to a doubly occupied Cu orbital. For low values of  $\Delta$ , the phase diagram is rather independent of  $U_d$ . Also, the effects of  $U_{pd}$  and  $U_d$  on the phase diagram on a qualitative level can be understood on general physical grounds: increasing these repulsions favors localization, inhibits the kinetic energy terms, and as a result the dependence of the energy on occupation is more flat, favoring phase separation. Although using ED we have only a few possible different densities, due to the small size of the cluster, the results for the compressibility at these densities agree qualitatively with the SB phase separation diagram. However there are some important differences in a quantitative level: a) there is no phase separation for  $U_{pd} \leq 2$ . b) For  $U_{pd} = 3$  there is a small island inside which the system phase separates in two phases, both with compositions inside the interval  $0 < x < 1$ . Some of these features can be seen in Fig. 10, where we show the chemical

potential  $\mu$  as a function of doping. In table I we list the densities for which the compressibility is negative (a sufficient but not necessary condition for phase separation) according to our ED results for different parameters.

#### IV. SUMMARY AND DISCUSSION

In this work, we have studied the effects of Cu-O Coulomb repulsion  $U_{pd}$  on valence instabilities and phase separation. Using a variational form of the cell method, we derive a one-band effective model with doping dependent parameters. This model has the form of a generalized Hubbard with correlated hoppings and nearest-neighbor repulsions. This approach allows us to study realistic values of the on-site Cu repulsion  $U_d \sim 10$  eV and is accurate enough for moderate values of  $U_{pd}$  and on-site O repulsion  $U_p$ . We obtain that for parameters near those derived using constrained-density-functional approximation [8], in particular  $U_{pd} \lesssim 1.3$  eV, the low- energy physics of the three-band Hubbard model can be well represented by the effective one-band model, with doping independent parameters. The effect of  $U_{pd}$  is merely to renormalize the effective parameters and there are neither valence instabilities nor phase separation.

For larger  $U_{pd}$  the effective parameters become strongly doping dependent and for  $U_{pd} \sim 3$  eV valence instabilities and phase separation appear. In agreement with previous weak-coupling results [16], we obtain that phase separation starts to occur for large doping values ( $x \sim 0.7 \pm 0.1$  according to the exact-diagonalization results or  $x \sim 1$  according to the slave-boson ones). The valence instability begins at  $x = 1$  in both treatments. This facts are in contrast to results of alternative previous strong-coupling approaches [12,14,18]. This is probably due to the facts that on the one hand, the slave-boson approximation produces an artificial increase of  $\chi_V$  at the metal-insulator transition ( $x = 0$ ), as discussed in section III, favoring PS at low  $x$ . On the other hand in Refs. [12,14,19], the  $U_{pd}$  and  $U_p$  terms were taken in a mean-field approximation, essentially equivalent to Hartree-Fock , (and since  $U_d$  is large, this induces an artificially large increase of the energy with doping), while in our present

treatment most of the  $U_{pd}$  term and a large part of the  $U_p$  one are treated exactly. In fact, we have verified that treating both terms in Hartree-Fock before performing the low-energy reduction to the one-band model (as was done in previous studies of the metal-insulator transition [25]), the results become qualitatively similar to those of Refs. [12,14].

## **V. ACKNOWLEDGMENTS.**

We are indebted to E. R. Gagliano for providing us the program for the exact diagonalization. One of us (M.E.S.) would like to thank M. Baliña for very helpful discussions. M. E. S. is supported by the Consejo Nacional de Investigaciones Científicas y Técnicas (CONICET), Argentina. A. A. A. is partially supported by CONICET.

## REFERENCES

- [1] V. J. Emery, Phys. Rev. Lett. **58**, 2794 (1987).
- [2] C. M. Varma, S. Schmitt-Rink, and E. Abrahams, Solid State Commun. **62**, 681 (1987).
- [3] P. B. Littlewood, C. Varma, and E. Abrahams, Phys. Rev. Lett. **63**, 2602 (1989).
- [4] F. C. Zhang and T. M. Rice, Phys. Rev. B **37**, 3759 (1988).
- [5] E. Dagotto and J. Riera, Phys. Rev. Lett. **70**, 682 (1993); E. S. Heeb and T. M. Rice, Europhys. Lett. **27**, 673 (1994).
- [6] C. D. Batista and A. A. Aligia, LT5375B.
- [7] Han Rushan, C. Chew, K. Phua, and Z. Gan, Phys. Rev. B **39**, 9200 (1989).
- [8] A. K. Mc Mahan, J. Annott, and R. Martin, Phys. Rev B **42**, 6268 (1990); M. Hybertsen, M. Schlüter, and N. Christensen, Phys. Rev B **39**, 9028 (1989); M. Hybertsen, E. Stechel, M. Schlüter, and D. Jennison, Phys. Rev. B **41**, 11068 (1990); J. Grant and A. Mc Mahan, Phys. Rev. Lett. **66**, 488 (1991).
- [9] E. R. Gagliano, A. G Rojo, C. A. Balseiro, and B. Alascio, Solid State Commun. **64**, 901 (1987); C. A. Balseiro, A. G. Rojo, E. R. Gagliano, and B. Alascio, Phys. Rev. B **38**, 9315 (1988); J. E. Hirsch, S. Tang, E Loh Jr., and D. J. Scalapino, Phys. Rev. Lett. **60**, 1668 (1988).
- [10] A. Sudbø, C. M. Varma, T. Giamarchi, E. B. Stechel, and R. T. Scalettar, Phys. Rev. Lett. **70**, 978 (1993).
- [11] I. E. Perakis, C. M. Varma, and A. E. Ruckenstein, Phys. Rev. Lett. **70**, 3867 (1993); C. M. Varma, Phys. Rev. Lett. **75**, 898 (1995).
- [12] J. Hicks, A. Ruckenstein, and S. Schmitt-Rink, Phys. Rev. B **45**, 8185 (1992)
- [13] Y. Bang, G. Kotliar, R. Raimondi, C. Castellani, and M. Grilli, Phys. Rev. B **47**, 3323

(1993).

- [14] R. Raimondi, C. Castellani, M. Grilli, Y. Bang, and G. Kotliar, Phys. Rev. B **47**, 3331 (1993); M. Grilli, R. Raimondi, C. Castellani, C. Di Castro, and G. Kotliar, Phys. Rev. Lett. **67**, 259 (1991).
- [15] P. B. Littlewood, Phys. Rev. B **42**, 10075 (1990).
- [16] N. Kothekar, K. Quader, and D. Allender, Phys. Rev. B **51**, 5899 (1995).
- [17] S. N. Coppersmith and P. B. Littlewood, Phys. Rev. B **41**, 2646 (1990).
- [18] D. Hirashima, Y. Ono, T. Matsuura, and Y. Kuroda, J. Phys. Soc. Jpn. **61**, 649 (1992).
- [19] S. Caprara and M. Grilli, Phys. Rev. B **49**, 10805 (1994).
- [20] H. B. Schüttler and A. J. Fedro, Phys. Rev. B **45**, 7588 (1992).
- [21] J. H. Jefferson, H. Eskes, and L. F. Feiner, Phys. Rev. B **45**, 7959 (1992)
- [22] L. F. Feiner, J. H. Jefferson, and R. Raimondi, preprint.
- [23] R. Hayn, V. Yushankhai, and S. Lovstov, Phys. Rev. B **47**, 5253 (1993), and references therein.
- [24] M. E. Simón, M. Baliña, and A. A. Aligia, Physica C **206**, 297 (1993).
- [25] M. E. Simón and A. A. Aligia, Phys. Rev. B **48**, 7471 (1993).
- [26] V. I. Belinicher and A. L. Chernyshev, Phys. Rev. B **49**, 9746 (1994); V. Belinicher, A. Chernyshev, and L. Popovich, Phys. Rev. B **50**, 13768 (1994).
- [27] A. A. Aligia, M. E. Simón, and C. D. Batista, Phys. Rev. B **49**, 13061 (1994).
- [28] C. D. Batista and A. A. Aligia, Phys. Rev. B **47**, 8929 (1993).
- [29] M. E. Simón and A. A. Aligia, Phys. Rev. B **52**, 7701 (1995).
- [30] R. Raimondi, L. Feiner, and J. Jefferson, Physica C **235-240**, 2203 (1994).

- [31] C. D. Batista and A. A. Aligia, Phys. Rev. B **48**, 4212 (1993); E **49**, 6436 (1994).
- [32] J. M. Eroles, C. D. Batista, and A. A. Aligia, BD5722.
- [33] G. Kotliar and A. E. Ruckenstein, Phys. Rev. Lett. **57**, 1362 (1986).
- [34] N. P. Ong, Z. Z. Wang, J. Clayhold, J. M. Tarascon, L. H. Greene, and W. R. McKinnon, Phys. Rev. B **35**, 8807 (1987); K. Sreedhar and P. Ganguly, Phys. Rev. B **41**, 371 (1990)

## FIGURE CAPTIONS

**Fig. 1:** On-site repulsion of the effective one-band model (Eq. 7) obtained by exact diagonalization (ED) (see text) as a function of hole doping  $x$  for different values of the Cu-O charge transfer energy ( $\Delta$ ) and Cu-O repulsion:  $U_{pd}=1$  (solid), 2 (dashed), 3 (dotted), 4 (dotted-dashed). Other parameters of the original three-band model (Eq. 2) are:  $U_d = 7$ ,  $U_p = 4$ ,  $t_{pd} = 1$ ,  $t_{pp} = .5$ .

**Fig. 2:** One particle on-site energy of the effective one-band model (Eq. 7) as a function of doping for different values of  $\Delta$  and  $U_{pd}$ . The three lower curves correspond to  $\Delta = 1$  and the other three to  $\Delta = 3$ . Other parameters as in Fig. 1.

**Fig. 3:** Nearest-neighbor hoppings of the effective one-band model (Eq. 7) as a function of doping for different values of  $\Delta$  ((a)  $\Delta = 1$ , (b)  $\Delta = 3$ ) and  $U_{pd}$ . Other parameters as in Fig. 1.

**Fig. 4:** Nearest-neighbor Coulomb repulsions of the effective one-band model (Eq. 7) as a function of doping for different values of  $\Delta$  and  $U_{pd}=1$  (solid), and 3 (dotted). Other parameters as in Fig. 1.

**Fig. 5:** Cu occupancy as a function of Cu-O charge transfer energy ( $\Delta$ ) for different dopings (indicated at the right of the corresponding curve) obtained by (a) exact diagonalization and (b) slave bosons. Other parameters are  $U_{pd} = 2$ ,  $U_d = 7$ ,  $U_p = 4$ ,  $t_{pd} = 1$ ,  $t_{pp} = 0.5$ .

**Fig. 6:** Same as Fig. 5 for  $U_{pd} = 4$ ,  $U_d = 10$ .

**Fig. 7:** Cu occupancy as a function of doping for different values of  $\Delta$  (indicated at the right of the corresponding curve) and  $U_d$ , obtained by slave bosons (SB). Other parameters are  $U_{pd} = 3$ ,  $U_p = 4$ ,  $t_{pd} = 1$ ,  $t_{pp} = 0.5$ .

**Fig. 8:** Valence susceptibility as a function of  $\Delta$  for the different positive dopings of Fig. 6 obtained by (a) exact diagonalization and (b) slave bosons. Other parameters as in Fig. 6.

**Fig. 9:** Phase-separation diagram  $\Delta$  vs.  $x$  obtained using SB for different values of  $U_d$  and  $U_{pd}$ . The dotted line indicates the first-order valence transition for  $U_{pd} = 4$  (for  $U_{pd} = 2, 3$  there are no first order VI transition). The solid squares represent the same obtained with

ED. Other parameters as in Figs. 1,5.

**Fig. 10:** Chemical potential as a function of doping for several values of  $\Delta$  calculated with (a) SB and (b) ED. Other parameters are  $U_{pd} = 3$ ,  $U_d = 7$ ,  $U_p = 4$ ,  $t_{pd} = 1$ ,  $t_{pp} = 0.5$ .

## VI. TABLE CAPTION

**Table I:** Values of the density  $n$  for which the compressibility is negative according to ED for different values of  $U_d$ ,  $U_{pd}$  and  $\Delta$ . Other parameters are  $U_p = 4$ ,  $t_{pd} = 1$ ,  $t_{pp} = 0.5$ .

$U_d$	$U_{pd}$	$\Delta$	$n$	$U_d$	$U_{pd}$	$\Delta$	$n$
7	3	0.5	0.4-0.8	10	3	0.5	0.4-0.8
7	3	1	0.4-0.8	10	3	2.5	0.4-0.8
7	3	2	—	10	3	3	—
7	4	0.5	0.2-1	10	4	0.5	0-1
7	4	1	0.4-1	10	4	1	0-1
7	4	2	0.6-1	10	4	2	0.4-1
7	4	3	—	10	4	3	0.6-1
				10	4	4	0.8-1
				10	4	5	—

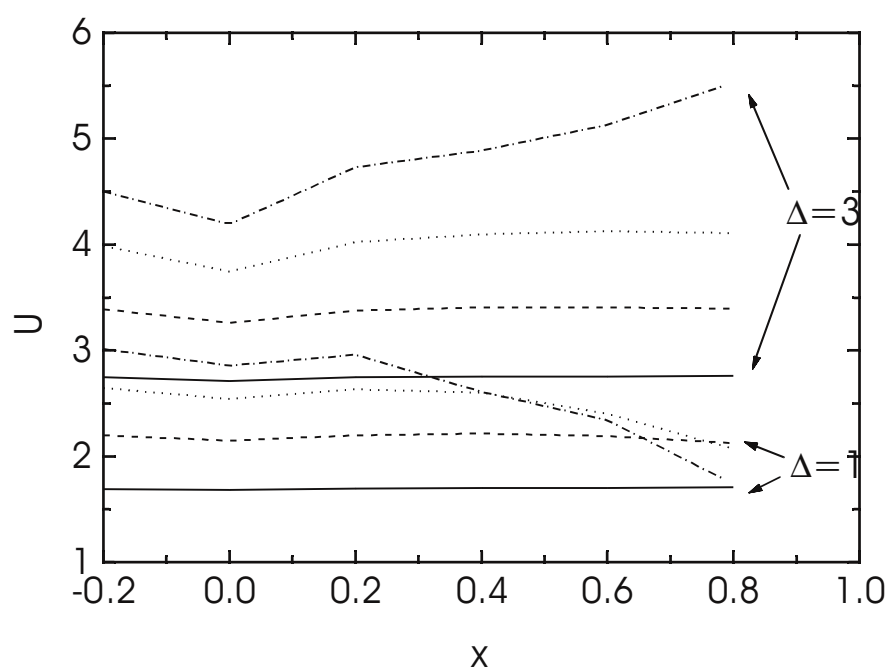


Fig. 1

Simon et al.

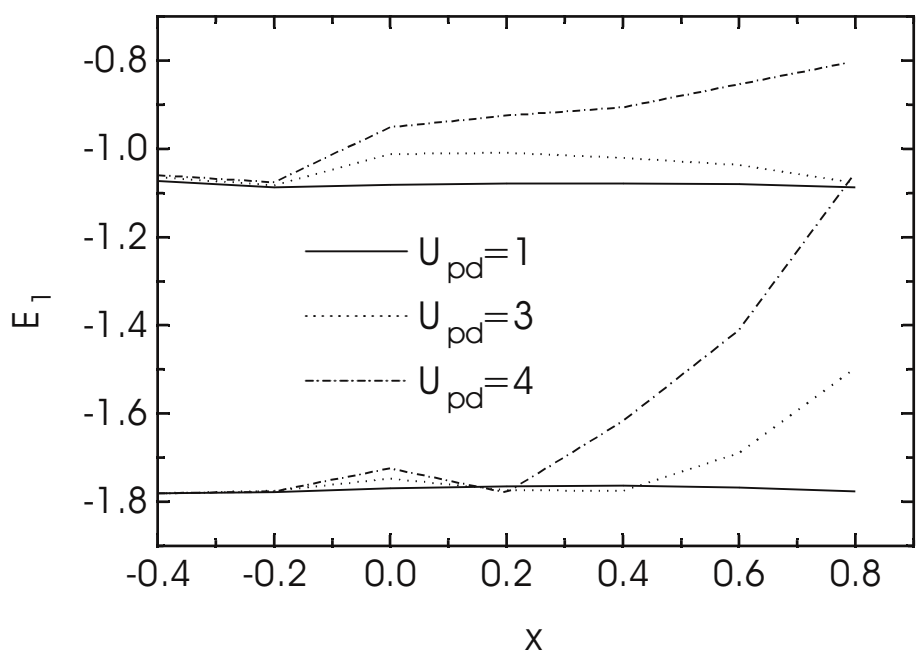


Fig. 2

Simon et al.

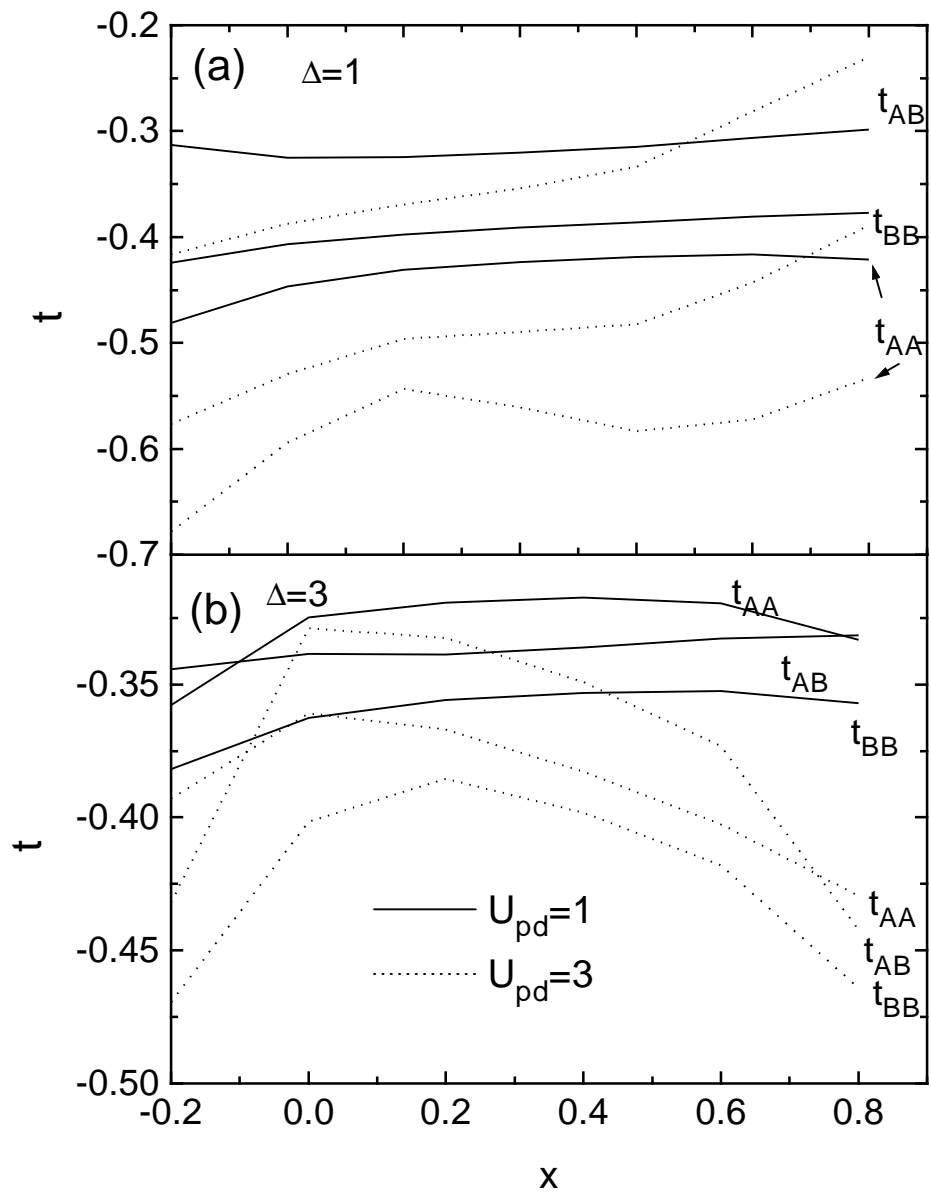


Fig. 3 Simon et al.

— B

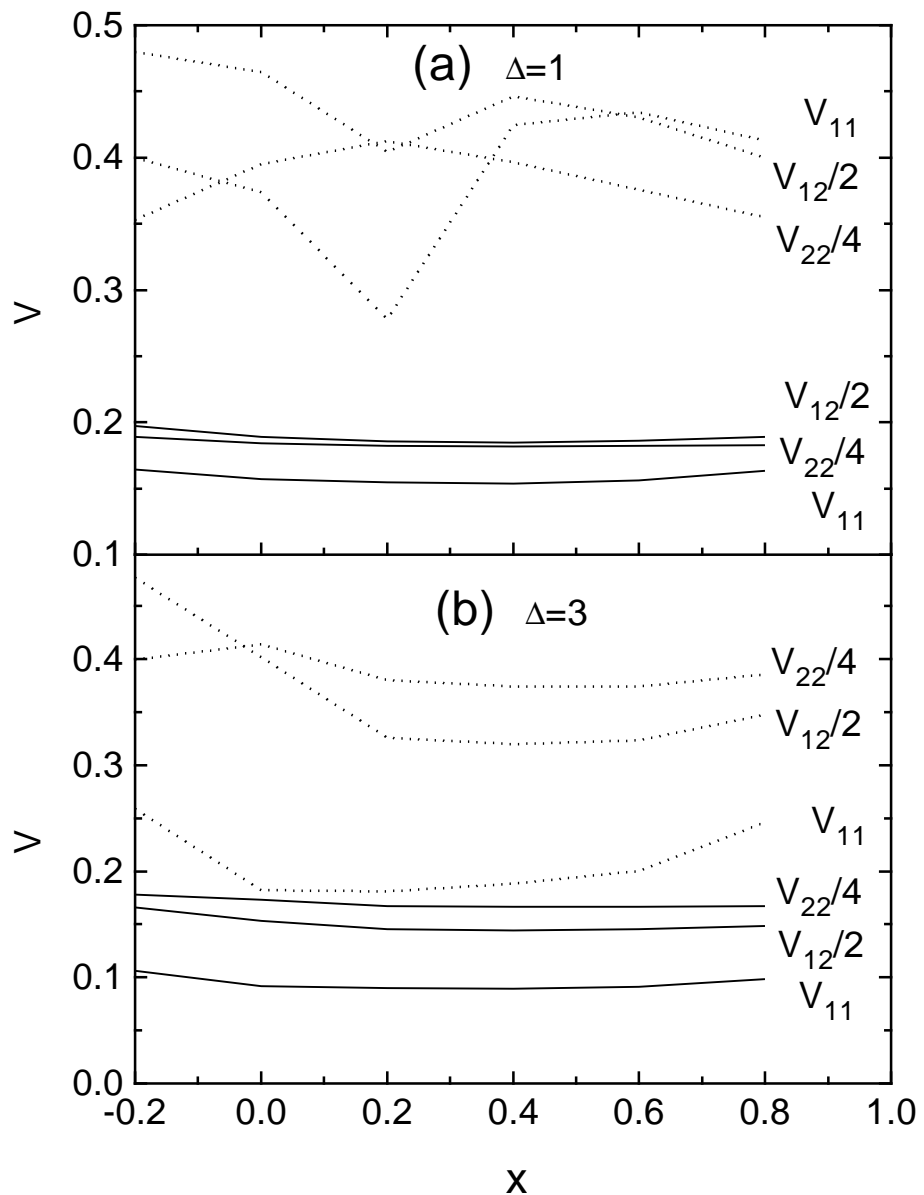


Fig. 4 Simon et al.

— B

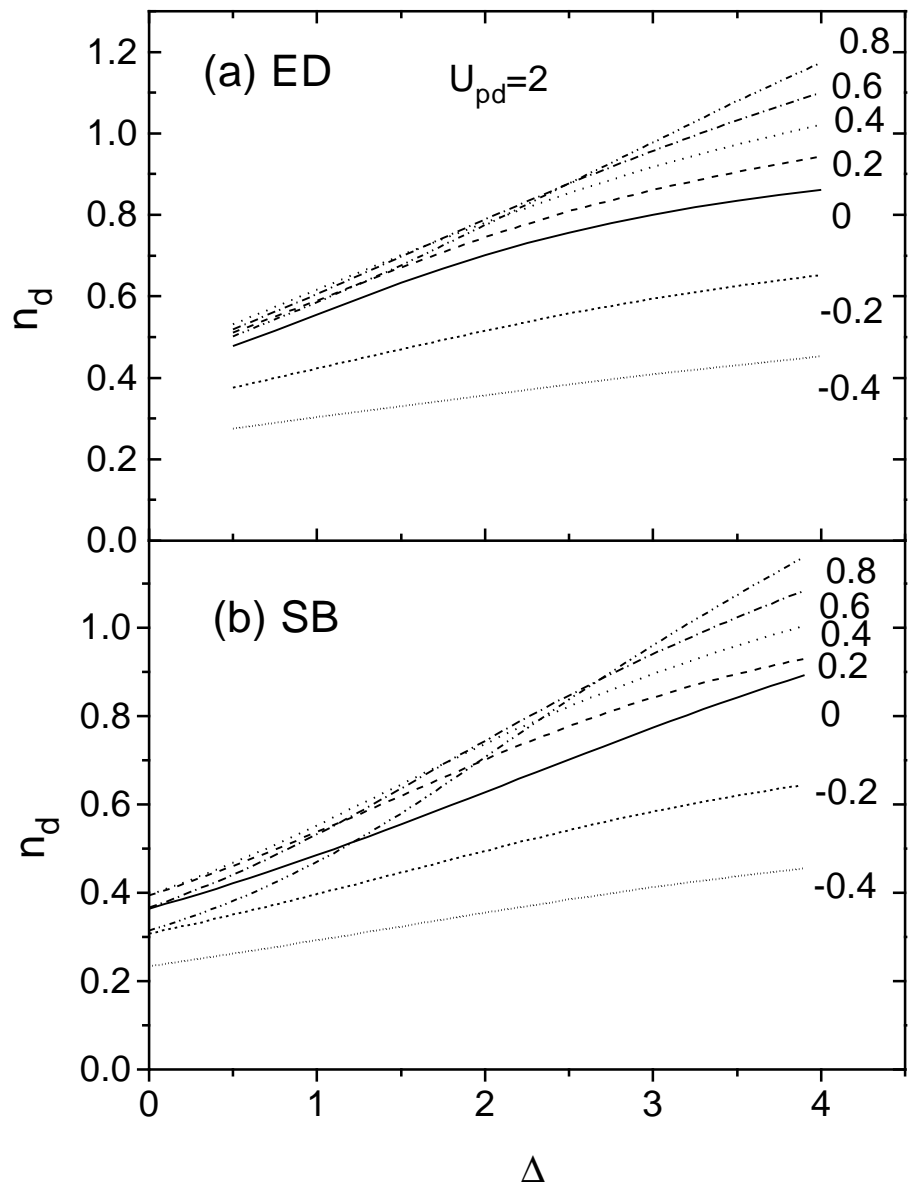


Fig. 5 Simon et al.

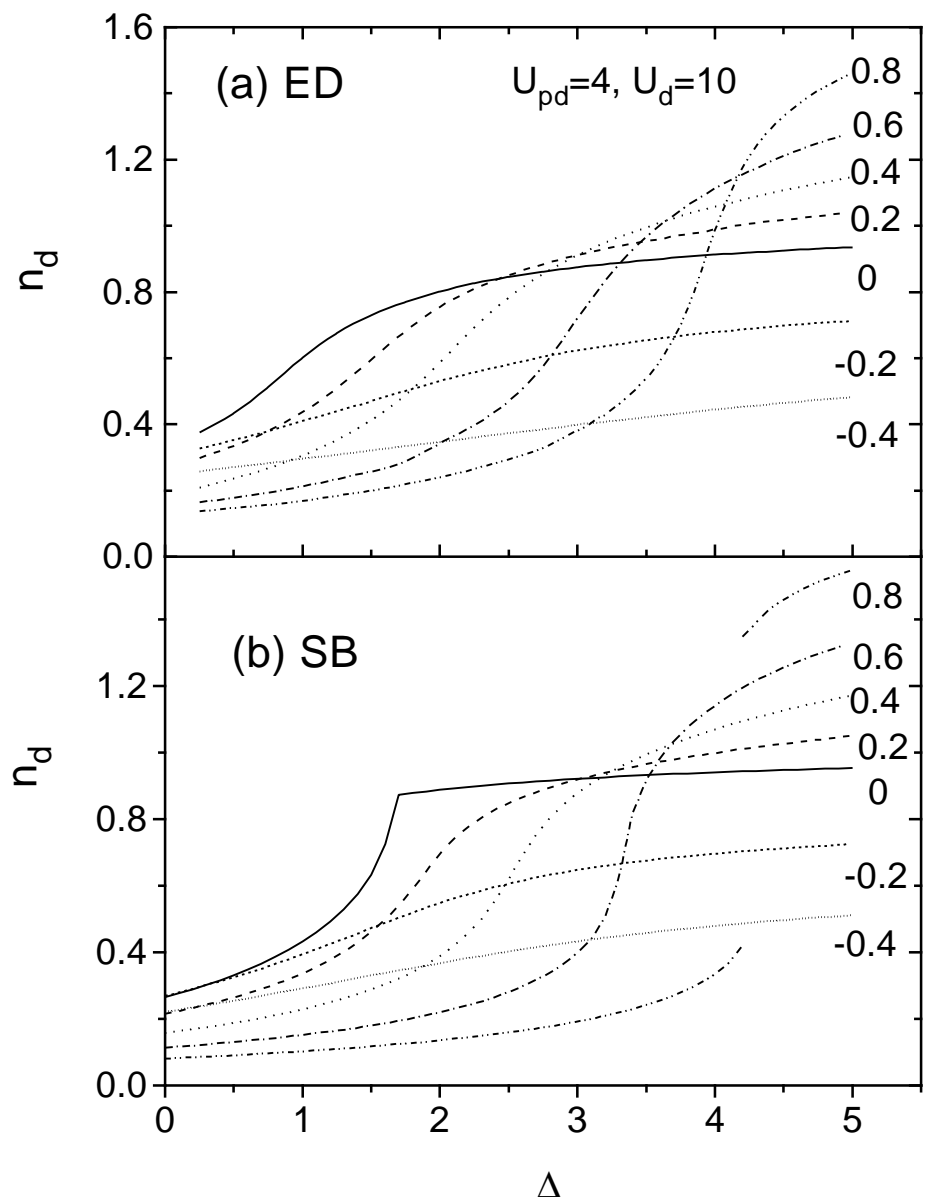
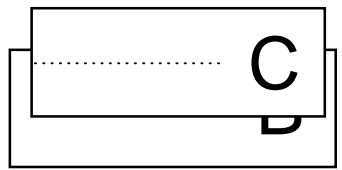


Fig. 6      Simon et al.

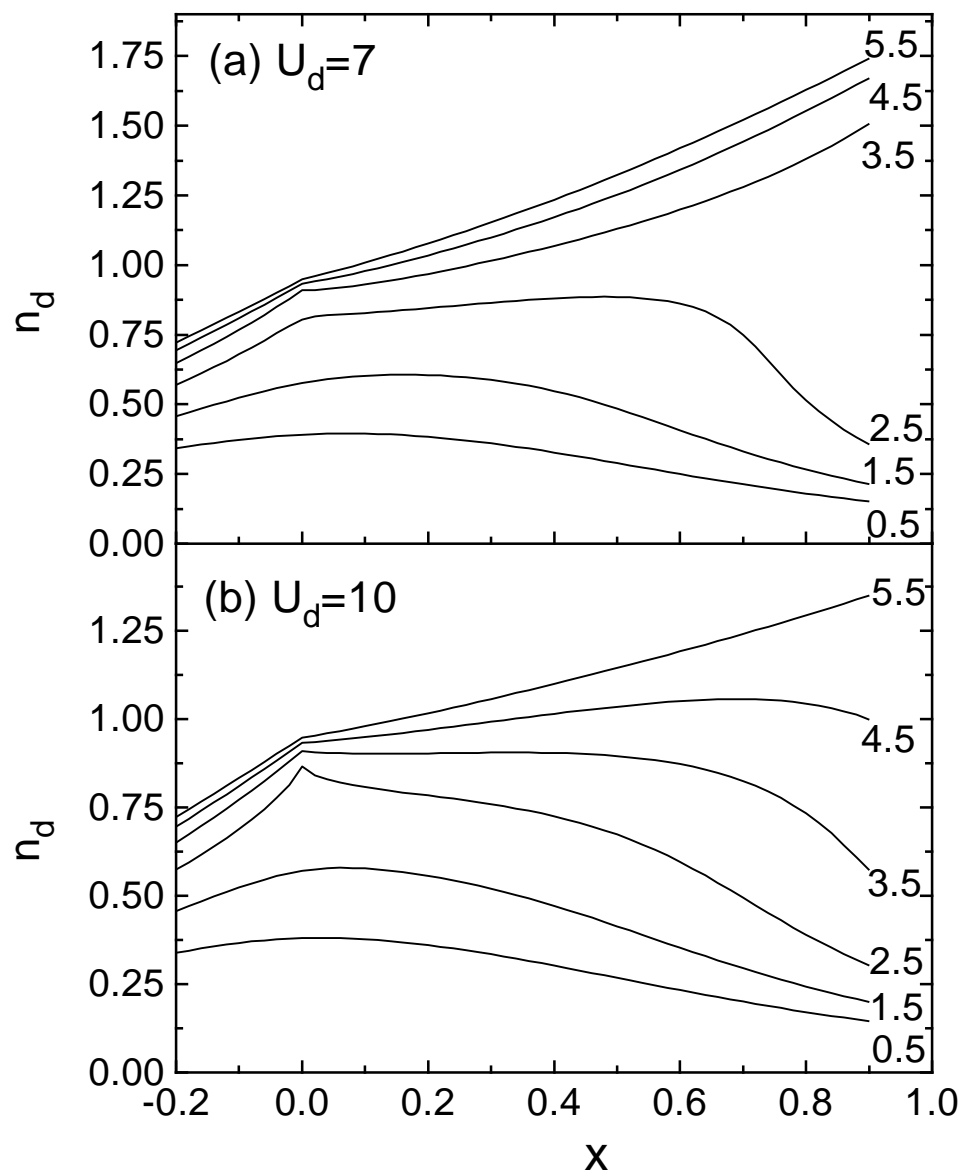


Fig. 7 Simon et al.

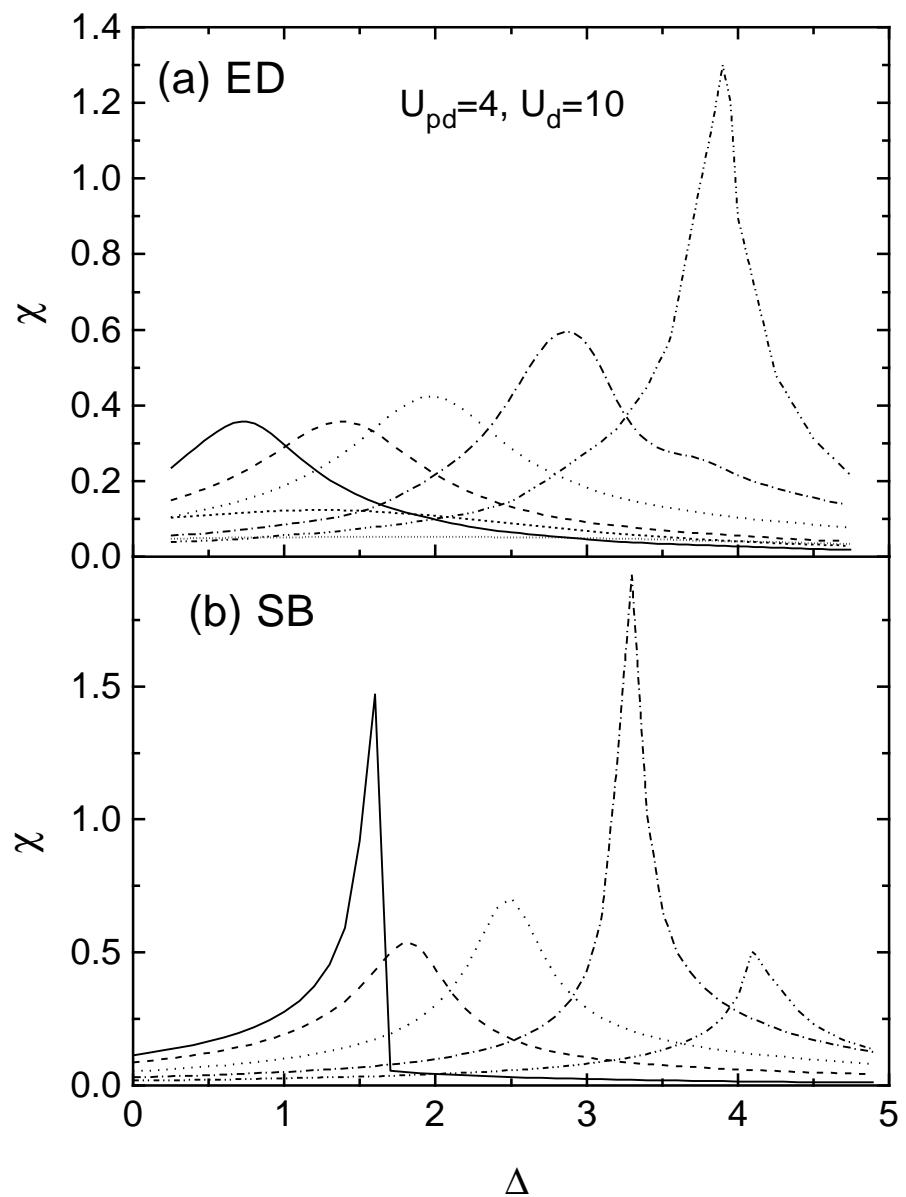
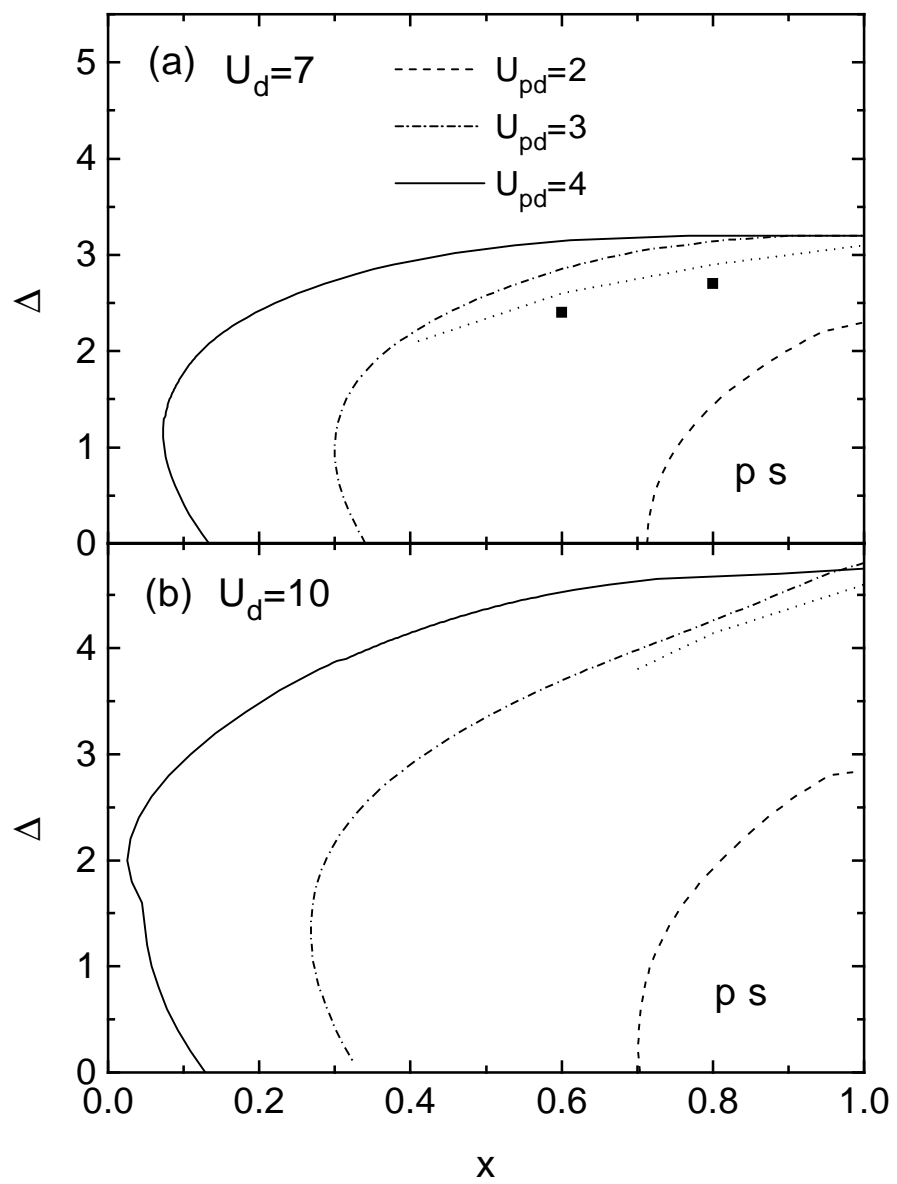


Fig. 8    Simon et al.



Simon et al . Fig 9

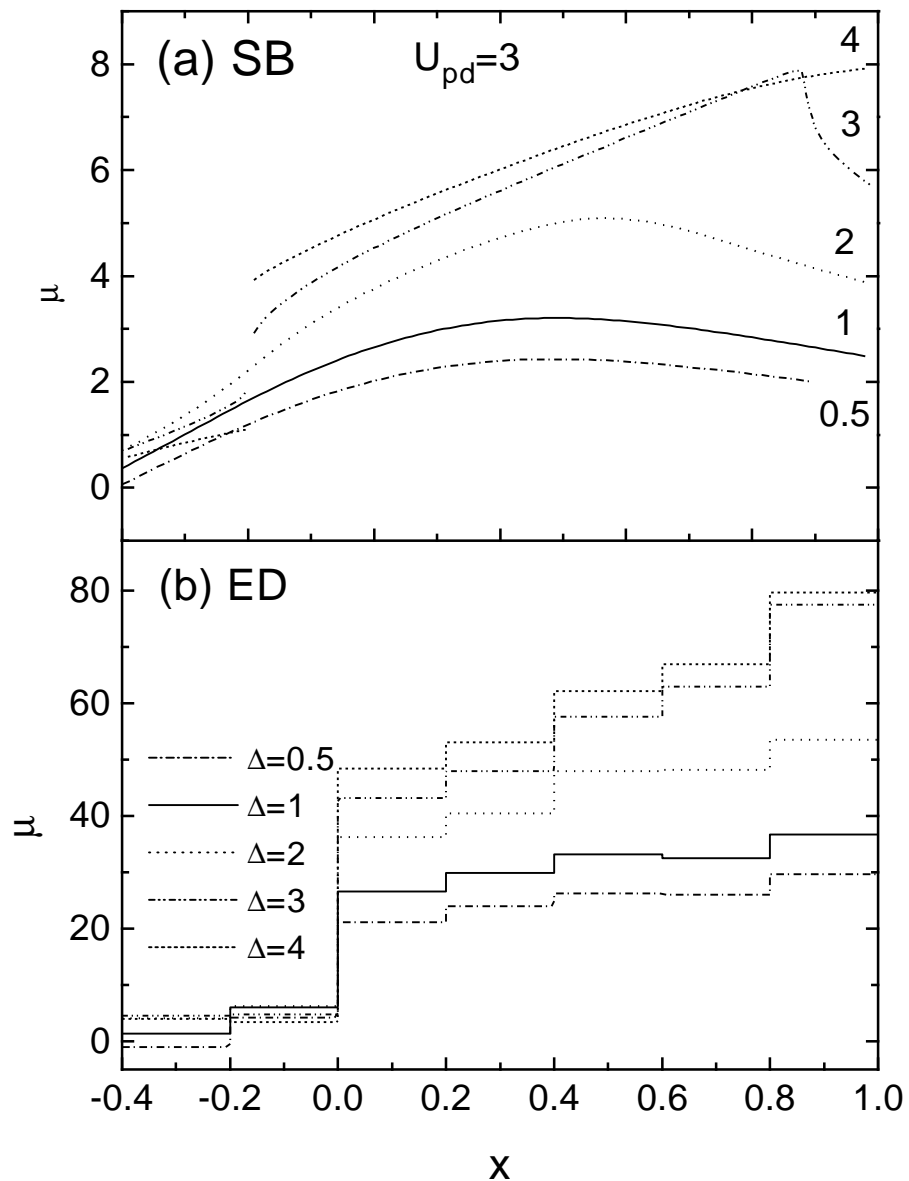


Fig. 10 Simon et al.